Surface Science 646 (2016) 288–297

Contents lists available at ScienceDirect

Surface Science

journal homepage: www.elsevier.com/locate/susc

Density functional theory study of O–H and C–H bond scission of methanol catalyzed by a chemisorbed oxygen layer on Cu(111)

Jonathan Li [a], Guangwen Zhou [b,*]

[a] Department of Physics, Applied Physics and Astronomy & Multidisciplinary Program in Materials Science and Engineering, State University of New York, Binghamton, NY 13902, USA
[b] Department of Mechanical Engineering & Multidisciplinary Program in Materials Science and Engineering, State University of New York, Binghamton, NY 13902, USA

ARTICLE INFO

Available online 28 November 2015

Keywords:
Methanol oxidation
Cu(111)
Cu_2O
Chemisorbed oxygen
Density-functional theory
Bond scission

ABSTRACT

Using the density-functional theory within the generalized gradient approximation, we have studied the partial oxidation of methanol on a Cu(111) surface covered with a chemisorbed oxygen layer that resembles a Cu_2O layer. Adsorption energies and geometries were computed for methanol, methoxy, hydroxymethyl and formaldehyde on both clean Cu(111) and Cu_2O/Cu(111) and electronic structures were computed for the reaction intermediates on Cu_2O/Cu(111). We also calculated the energy barrier for partial oxidation of methanol to formaldehyde on Cu_2O/Cu(111). These results show that the Cu_2O monolayer slightly lowers the stability of each of the surface adsorbates and the oxygen strongly promotes hydrogen dissociation by lowering the energy barrier of methanol decomposition and causing the spontaneous dissociation of methanol into methoxy.

© 2015 Elsevier B.V. All rights reserved.

1. Introduction

There has been an increasing need for alternative energy sources due to the diminishing supply of petroleum and their pollution problems [1]. Methanol is the smallest alcohol molecule, and is being studied as a sustainable form of energy. Methanol is often transformed into hydrogen to be used as a clean fuel [2]. Hydrogen can be obtained from methanol by a variety of processes, such as methanol decomposition [3,4]

$$CH_3OH = CO + 2H_2,$$

methanol oxidation [5–7]

$$CH_3OH + \frac{O_2}{2} = CO_2 + 2H_2,$$

and methanol steam reforming [8,9]

$$CH_3OH + H_2O = CO_2 + 3H_2.$$

Methanol decomposition, the most basic way to generate hydrogen, is also an endothermic reaction, and is harmful to the environment and poison for the fuel cell. Steam reforming combines methanol with water and gives the highest hydrogen concentration [10]. However, its major disadvantage is its endothermicity, requiring external heating. In comparison, hydrogen can be produced with no need of external heating by using the partial oxidation of methanol (POM) with oxygen or air.

Industrially, methanol synthesis and decomposition are promoted by Al_2O_3-supported Cu/ZnO catalysts [11]. Although Cu is generally believed to require low-temperature POM, the exact identity of the active species of Cu is as yet unclear. Metallic copper is believed to be the active component in Cu-based catalysts in methanol oxidation, steam reforming, and decomposition [10,12]. However, conflicting reports exist where no general correlation between the activity and the surface area of metallic Cu was reported. For example, Huang et al. [13] proposed that Cu^+ species help to increase the activity of Cu-based catalysts, where both Cu^0 and Cu^+ species are essential for hydrogen generation from CH_3OH and the activity of catalyst is dependent on the ratio of Cu^+/Cu^0. Oguchi et al. [14] stated that the active Cu species in Cu-based catalysts is only Cu_2O during methanol oxidation.

There have been many theoretical studies on methanol oxidation on low-index Cu surfaces. Sakong et al. focused on the POM on clean and oxygen-covered Cu(100) and Cu(110) using the density-functional theory (DFT) and kinetic Monte Carlo (kMC) [15–17]. Methanol has been studied on clean Cu(111) modeled by a finite cluster [18] or by a periodic slab [12,19,20] and on clean Cu(100) by a finite cluster [21]. These studies have dealt mostly with clean surfaces, and the few oxygen covered surface studies mentioned dealt with isolated oxygen atoms rather than a chemisorbed layer. The theoretical studies [15,17–19] have shown that decomposition of methanol on Cu is strongly promoted by the presence of surface oxygen, which is in accordance with experimental measurements [22–24].

There have also been DFT studies on methanol oxidation on the surfaces of bulk oxides such as V_2O_5 [25], Co_3O_4 [26], and oxygen-

* Corresponding author.
E-mail address: gzhou@binghamton.edu (G. Zhou).

http://dx.doi.org/10.1016/j.susc.2015.11.012
0039-6028/© 2015 Elsevier B.V. All rights reserved.

covered Cu(100) and Cu(110) [15–17]. Boulet et al. found that the oxygen atoms on the oxide surface serve several purposes. The adsorption of methanol is stronger on a partially reduced surface because it can form hydrogen bonds. In addition, the formation of methoxy to formaldehyde requires the vanadyl oxygen vacancy to be filled by a diffused oxygen atom in the lattice, indicating that surface oxygen atoms are needed for the oxidation of methanol on V_2O_5 [25]. Lv et al. studied methanol oxidation on Co_3O_4 and found that the dissociated hydrogen atoms of methanol prefer to adsorb on the oxygen atoms of the oxide surface [26]. Sakong et al. found that the oxygen-covered Cu surfaces promote the methanol oxidation and help remove the surface hydrogen atoms via water desorption [15–17]. These studies focused on the surfaces of bulk crystals and adsorbed oxygen atoms. Here we report a DFT study of methanol oxidation on an oxygen chemisorption reconstructed surface, which is an oxide monolayer on a metallic slab. Since methanol oxidation is affected by both surface structure and surface chemistry, the chemical reactions on an oxygen chemisorbed surface may differ than on the surfaces of bulk oxide crystals and on surfaces with individually adsorbed oxygen atoms.

It is well known that Cu surfaces exposed to oxygen will initially form a chemisorbed oxygen layer, and a surface reconstruction is therefore expected. The O/Cu(111) system has been studied both experimentally [27–36] and theoretically [37–40], and experimental studies have shown that oxidation of the Cu(111) surface is extremely complex. Surface geometries are described as the "44" structure and a "29" structure that resemble a Cu_2O monolayer. Only a few theoretical studies have been conducted on the complex Cu(111) oxide surfaces; Soon et al. studied the thermodynamics and stability of the oxide layers [38–40], and Yang et al. studied the autocatalytic reduction of a Cu_2O(111) layer on Cu(111) [41]. Although the "44" and "29" structures have a large super cell, the O/Cu(111) system can be modeled well by using a smaller model shown in the aforementioned studies. In this work, we employed DFT to study partial oxidation of methanol on a Cu_2O chemisorbed oxygen layer on Cu(111). By comparing with clean Cu(111), we elucidate the microscopic origin of the effect of the oxygen chemisorption layer on the improved surface reactivity toward catalytic POM.

2. Computational methods

The DFT calculations were performed using the Vienna ab-initio simulation package (VASP) [42–45] with the PW91 generalized gradient approximation (GGA) [46,47] and projector augmented wave (PAW) [48,49] potentials. We chose to use the GGA using PW91 exchange-correlation functional due to its efficiency, computational time and use in previous studies. PW91-GGA has been used in recent studies for chemical reactions regarding oxygen-covered Cu surfaces [15,16,41] and also for methanol decomposition [15,16,19,50]. Similar to previous studies on methanol oxidation calculations using DFT [15, 16], a cutoff energy of 350 eV was adopted in our calculations. We also performed a separate cutoff energy test, using cutoff energies of 350 eV and 400 eV, by adsorbing methanol onto the surface of our Cu_2O/Cu structure model and found that the difference in methanol adsorption energy was only 0.03 eV. We have performed both spin and non-spin polarized calculation tests to ensure that the spin did not have an effect in describing the transition state and found that there was no significant difference in the results. However, there have been DFT studies of methanol dissociation where spin-polarization was considered, such as on V_2O_5 [25] and Co_3O_4 [26]. These studies require spin polarization calculations due to the magnetic properties of the catalyst, as O vacancies (which can be formed by methanol oxidation) cause V_2O_5 to become ferromagnetic [51] and Co_3O_4 is antiferromagnetic, while our catalyst is diamagnetic. Therefore, no spin polarization effect was considered in our calculations.

The Brillouin-zone integration was performed using $(3 \times 3 \times 1)$ K-point meshes based on Monkhorst–Pack grids [52] and with broadening of the Fermi surface according to Methfessel–Paxton smearing technique [53] with a smearing parameter of 0.2 eV. To test the accuracy of the 0.2 eV smearing parameter, we calculated the adsorption energy of methanol on the Cu_2O/Cu(111) surface using 0.2 eV and 0.05 eV smearing and found that the change in adsorption energy was less than 0.01 eV. The total energy of the Cu_2O/Cu(111) slab only changed by 0.5 meV per atom. We calculated the lattice constant of Cu to be 3.64 Å, which is in good agreement with previous calculations [54–56]. The flat Cu(111) surface was simulated by a three-layer 4×4 slab model, and one monolayer of Cu_2O was adsorbed on Cu(111) to model Cu_2O/Cu(111). The bottom two layers of the Cu surface were fixed at the lattice position and all other atoms were allowed to fully relax during optimization until all force components acting on the atoms are below 0.015 eV/Å. Successive slabs are separated by a vacuum region of 12 Å.

We applied the climbing image nudged elastic bands (CI-NEB) method [57] to calculate the reaction barriers, where we used seven intermediate images between the initial and final states. We calculated the adsorption energy of both oxygen atoms and molecules on the surface of our slab models. The adsorption energy E_{ads} was calculated using the following equation

$$E_{ads} = \frac{1}{N_{ads}}\left(E_{ads}^{tot} - E_{ref} - E_{gas}\right),$$

where E_{ads}^{tot} is the total energy of the system that includes both the Cu–O system with the adsorbate, or the pure Cu system with adsorbate and E_{ref} is the energy of the structure that we used as a reference to compare the relative stability, and more specifically, it is the total energy of the system without an adsorbate on the surface. E_{gas} is the energy of a molecule in its gas phase, calculated by placing an isolated molecule in a box, and N_{ads} is the number of molecules newly adsorbed into the system, which is equal to 1 throughout this work. E_{gas} for an oxygen atom is calculated by taking half the energy of an isolated oxygen molecule E_{O_2}. Although the adsorption energies calculated using the above equation should be given with respect to stable gas-phase species (in our case, CH_3OH was used, as well as O_2 as reference for atomic O adsorption and H_2 as reference for atomic H adsorption), we found that the convention was to continue to use the above equation for the adsorption energies of the reaction intermediates, regardless of them being radicals [15,58–60] and we thus followed the convention in order to make comparable results. The atomic structures and charge difference are visualized using the VESTA package [61,62].

3. Results and discussion

3.1. Structure of the Cu_2O/Cu(111) surface

The surface oxide phases "44" and "29" are thought to resemble the primary structure of a Cu_2O(111) monolayer, consisting of a tri-layer repeat unit with each Cu layer packed in between two layers of oxygen atoms. Jensen et al. [28,29] and Matsumoto et al. [27] suggest the "44" structure originates from a distorted Cu_2O(111) layer, which has the same honeycomb structure as the Cu_2O(111) surface and coordinatively under-saturated Cu atoms removed, grown epitaxially on Cu(111). "44" and "29" have unit cell surface areas 44 and 29 times that of the Cu(111) unit cell. The "44" and "29" structures would require an enormous computational effort to perform DFT calculations due to their large sizes. Therefore, we have downsized the model to a (4×4) supercell to imitate the superoxide structures observed experimentally. We perform calculations to determine the similarity of geometric properties of our downsized model with those of bulk Cu_2O.

The Cu_2O monolayer on the Cu(111) model is shown in Fig. 1(a) and the unit cell lines are shown within the solid black border. The periodicity of the honeycomb structures is measured to be 0.60 nm, corresponding to the lattice spacing of the Cu_2O(111) layer on

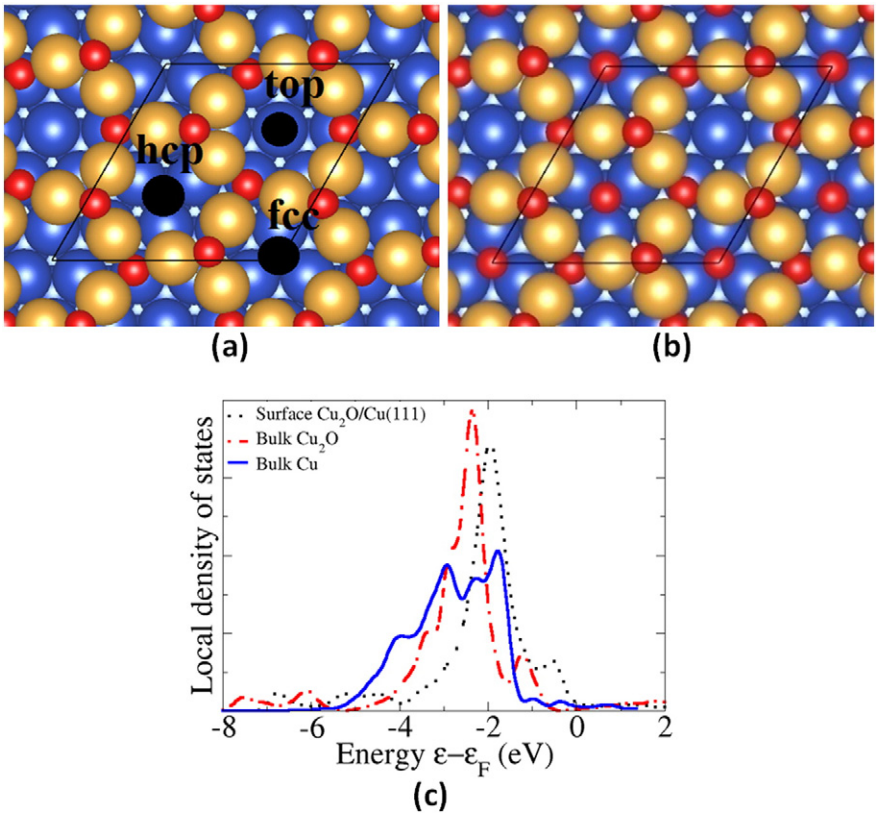

Fig. 1. The structural model of the $Cu_2O(111)$ layer on Cu(111): (a) Surface with black circles representing the potential adsorption sites for an oxygen atom, labeled hcp, fcc and top. (b) Surface with stable oxygen atoms chemisorbed at the fcc and hcp sites. The yellow balls represent Cu atoms that make up the $Cu_2O(111)$ layer, the blue balls represent Cu atoms under chemisorbed layer, and the smaller red atoms represent the oxygen atoms. The border is the unit cell we used in all of our surface calculations. (c) Comparison of density of states of the d structure of a Cu atom on the $Cu_2O/Cu(111)$ surface, bulk Cu_2O and bulk Cu. The units for the density of states are in arbitrary units.

Cu(111). We compare our Cu_2O-layer with that of bulk Cu_2O and a previous theoretical study. We found the thickness of our O–Cu–O layer to be 1.13 Å, agreeing well with a previous calculation of 1.20 Å [38] and also the thickness found in bulk $Cu_2O(111)$ of 1.22 Å. We found the average Cu–O bond length to be 1.83 Å, the same as the previous calculation [38] and very close to that of bulk Cu_2O of 1.85 Å, and the average bond angle to be 109.7° compared with 109.0° in bulk Cu_2O.

There are two types of oxygen species in our structural model, chemisorbed oxygen and lattice oxygen within Cu_2O. The black circles in Fig. 1(a) show the possible adsorption sites for additional oxygen atoms: fcc, hcp and top. These adsorption sites are on the surface of the Cu layer that are exposed in the centers of the hexagonal structure of $Cu_2O(111)$. To determine the stability of the chemisorbed oxygen, we calculated the adsorption energy of the oxygen at each adsorption site. An oxygen on the fcc and hcp positions has adsorption energies of −1.59 eV and −1.51 eV, respectively. The fcc hollow site is more stable than the hcp hollow site by 0.08 eV, which agrees well with 0.05 eV calculated by Yang et al. [63] and less than the difference of 0.15 eV calculated by Soon et al. [38]. The adsorption energy of oxygen atoms on both hcp and fcc at the same time is −2.97 eV. An oxygen atom on the top site is unstable and thus is not further investigated. Therefore, we considered chemisorbed oxygen atoms at both fcc and hcp sites for our structure model for all of our calculations, shown in Fig. 1(b). While the "44" and "29" structures have much larger supercells, we find that our model matches well in geometry and is a reasonable model to represent the O/Cu(111) system and we use the term $Cu_2O/Cu(111)$ to refer to the surface of our $Cu_2O(111)$ layer on Cu(111) for the remainder of this paper.

We now consider the electronic structure by calculating the local density of states. Fig. 1(c) shows the LDOS for a Cu atom on the $Cu_2O/Cu(111)$ surface, in bulk Cu_2O and in bulk Cu. There is significant narrowing of the band of Cu in the $Cu_2O/Cu(111)$ oxide layer, which is very similar to the bulk Cu_2O. The Cu atoms in the open structure of the $Cu_2O/Cu(111)$ also have lower coordination compared to the bulk Cu. We found that the $Cu_2O/Cu(111)$ surface oxide electronic structure has similar features to the bulk Cu_2O and resembles a semiconductor, rather than metallic Cu.

3.2. Structure of surface adsorbates on $Cu_2O/Cu(111)$ and clean Cu(111)

Detailed DFT calculations have been performed to determine the minimum energy structures of the reaction intermediates of partial methanol oxidation. As the surface structure of our $Cu_2O/Cu(111)$ is very complex, there is a large number of possible adsorption sites. We have determined the minimum energy structures of the molecules by adsorbing them on the surface of the $Cu_2O/Cu(111)$ surface at the top and bridge sites of the Cu atoms of the Cu_2O lattice, and also on top of the lattice and chemisorbed oxygen atoms and we only report the most stable configurations. As O–H bond scission in methanol results in methoxy, O–H bond scission in methoxy results in formaldehyde and C–H scission results in hydroxymethyl, the reaction intermediates considered in our calculations are methanol, methoxy, hydroxymethyl and formaldehyde. Many studies have shown that methanol decomposition starts with O–H bond breaking on transition metal surfaces. However, Greeley et al. determined that methanol decomposition on clean Pt(111) is initiated by the breaking of the C–H bond [50]. There have also been DFT studies of methanol reactions on different metal oxide surfaces. Vo et al. studied methanol adsorption and decomposition on $ZnO(10\bar{1}0)$ and found that methanol is most stable on top of a Zn atom bonded by its O atom and first dissociates to methoxy [64]. Calatayud et al. found that dissociation of methanol on the $SnO_2(110)$

surface is initiated by the C–O bond scission [65]. On the $Ti_2O(110)$ surface, methanol interacts with both the bridging oxygen and Ti atom, and dissociates to methoxy with a low energy barrier [66]. These studies indicate that the methanol dehydrogenation mechanism is dependent on the surface composition and structure.

It is necessary to explore the initial C–H and O–H bond scission of methanol on Cu_2O/Cu(111) and clean Cu(111). The adsorption geometries of methanol, methoxy, hydroxymethyl and formaldehyde in their most stable configurations and their adsorption energies are listed in Table 1. Our calculations reveal two stable configurations of methanol, O-adsorbed and H-adsorbed. Both will be discussed in the following sections.

3.2.1. Methanol (CH_3OH)

3.2.1.1. O-adsorbed methanol. The side and top views of methanol adsorbed on the Cu_2O/Cu(111) surface are shown in Fig. 2(a, b). The closed-shell species methanol (CH_3OH) is weakly bonded on top of a Cu atom by the molecule's oxygen atom to both clean Cu(111) and Cu_2O/Cu(111) layer, with an adsorption energy of 0.38 eV and 0.23 eV, respectively. The distances from the C and O in the O–H bond to the closest Cu atom on the surface are 3.30 Å and 2.29 Å for the clean Cu(111) and 3.61 Å and 2.52 Å for Cu_2O/Cu(111). The hydroxyl bond (O–H) is oriented slightly parallel to the surface and the C–O bond is tilted upright for both the clean Cu(111) and the Cu_2O/Cu(111) surface. Methanol is adsorbed slightly stronger to the clean Cu(111), having a shorter O–Cu distance and a higher adsorption energy. Methanol adsorbed by its O atom on top of a surface O atom is unstable and reorients itself so that the H atom in the hydroxyl bond is bonded to the surface O atom, which will be discussed later in Section 3.2.1.2. If methanol is placed in an upright or horizontal position on top of a Cu atom, it will orient itself to be tilted after geometric optimization.

We can study the electronic structure by plotting the local density of states for our system. Fig. 2(c) shows the local density of states of the O atom in methanol and the Cu atom of the Cu_2O/Cu(111) that it bonds to. The peaks of the p-orbital of the O atom are slightly downshifted. However, the peaks are still well defined except for the higher state orbital. The peaks are still located relatively close to their gas phase positions after adsorption. The peak of the d-structure of the Cu atom that methanol bonds to is hardly changed after methanol adsorption, as its peak does not change shape or downshift. Since the H atom of methanol hydroxyl bond is relatively close to the surface, we also study its electronic structure to determine if it has any significant bonding with the surface. The H atom in the hydroxyl bond is 2.02 Å away from an O atom on the Cu_2O/Cu(111), which is less than the distance between the methanol's O atom and a surface Cu atom on the Cu_2O/Cu(111). Fig. 2(d) shows the local density of states of the H atom in the hydroxyl bond and the O atom on the Cu_2O-layer under it. The plot shows that the O atom is not changed, and the s-orbital of H atom changes even less than the O atom in methanol does. While there is a slight downshift in the H s-orbital, the peaks are still well defined and very close to their gas phase positions. The charge density difference plot is shown in Fig. 2(e) and does not show significant charge transfer between surface O atom and the H atom of methanol. We conclude that methanol is physisorbed on both Cu(111) and Cu_2O/Cu(111) based on its low adsorption energy and large bond distance. The lack of change of local density of states in O-adsorbed methanol on Cu_2O/Cu(111) further show that the interaction between methanol and the chemisorbed oxygen layer is weak.

3.2.1.2. H-adsorbed methanol. The side and top views of methanol adsorbed on the Cu_2O/Cu(111) surface are shown in Fig. 3(a, b). The closed-shell species methanol (CH_3OH) is weakly bonded on top of an O atom by the molecule's H atom in the hydroxyl bond on the surface of Cu_2O/Cu(111), with an adsorption energy of −0.20 eV. Although this configuration is less stable than the O-adsorbed methanol, we still consider this for further calculations to examine the differences between the two states. The distances from the H and O in the O–H bond to the closest O atom on the surface are 1.87 Å and 2.85 Å. The hydroxyl bond (O–H) is oriented almost completely perpendicular to the surface and the C–O bond is slightly tilted from a parallel position. Although the O-adsorbed methanol is positioned further from the surface, the H-adsorbed methanol is slightly less stable.

The electronic structure can be revealed by plotting the local density of states for our system. Fig. 3(c) shows the local density of states of the H atom of the hydroxyl bond in methanol and the surface O atom of Cu_2O/Cu(111) that it bonds to. The peaks of the p-orbital of the surface O atom are hardly changed after methanol adsorption. The peaks of the s-orbital of the H atom shift slightly, but still have their well defined shape and are close to their gas phase positions. Fig. 3(d) shows little charge transfer between the surface O atom and the H atom of the methanol. Like the O-adsorbed methanol, the H-adsorbed methanol is only weakly bonded to the surface.

3.2.2. Methoxy (CH_3O)

The closed-shell species methoxy (CH_3O) is strongly bonded to multiple Cu atoms by the molecule's O atom to both the clean Cu(111) and Cu_2O/Cu(111) surfaces, having an adsorption energy of −2.66 eV and −1.88 eV, respectively. The side and top views of the molecule adsorbed on the Cu_2O/Cu(111) surface are shown in Fig. 4(a, b). The distances from the C and O atoms to the closest Cu atom on the surface are 3.16 Å and 2.04 Å for Cu(111) and 3.04 Å and 2.02 Å for Cu_2O/Cu(111). The C–O bond in CH_3O on clean Cu(111) is almost completely upright, but is slightly tilted when on the Cu_2O/Cu(111) surface. The O atom of the molecule is bonded to the surface at the fcc site for the clean Cu(111) surface. For the Cu_2O/Cu(111) surface, the fcc site does not exist. Instead, the most stable configuration is the O atom of the molecule bonded to the surface at the bridge site of two Cu atoms as shown in Fig. 4(b). A methoxy placed at the top of a Cu atom will spontaneously shift toward the bridge site where there is an O atom in the lower layer of the O–Cu–O tri-layer of the Cu_2O monolayer. The driving force for the migration of methoxy toward the bridge site is the instability of methoxy on top of a Cu atom, as well as the preference of the O atom in the open-shell methoxy to be coordinated with more than one copper atom. For example, on a clean Cu(111) surface, methoxy prefers to adsorb onto the fcc site.

The local density of states of the O atom in methoxy and one of the Cu atoms of Cu_2O/Cu(111) that it bonds to is plotted in Fig. 4(c). In the gas phase, methoxy is an open-shell radical. The peaks of the p-orbital of O have significantly broadened upon interaction with the surface and the single larger peak has split as well. This hybridization

Table 1
Adsorption energies and adsorption configurations of the reaction intermediates on both clean Cu(111) and Cu_2O/Cu(111) layer.

Reaction intermediate	E_{ads} (eV) on Clean Cu(111)	E_{ads} (eV) on Cu_2O/Cu(111)	Bonding on Clean Cu(111)	Bonding on Cu_2O/Cu(111)
CH_3OH	−0.38	−0.23	O–top	O–top Cu
		−0.20		H–top O
CH_3O	−2.66	−1.88	O–fcc	O–bridge Cu
CH_2OH	−1.51	−1.36	C–top	C–top Cu
CH_2O	−1.92	−0.92	O–top	O–top Cu

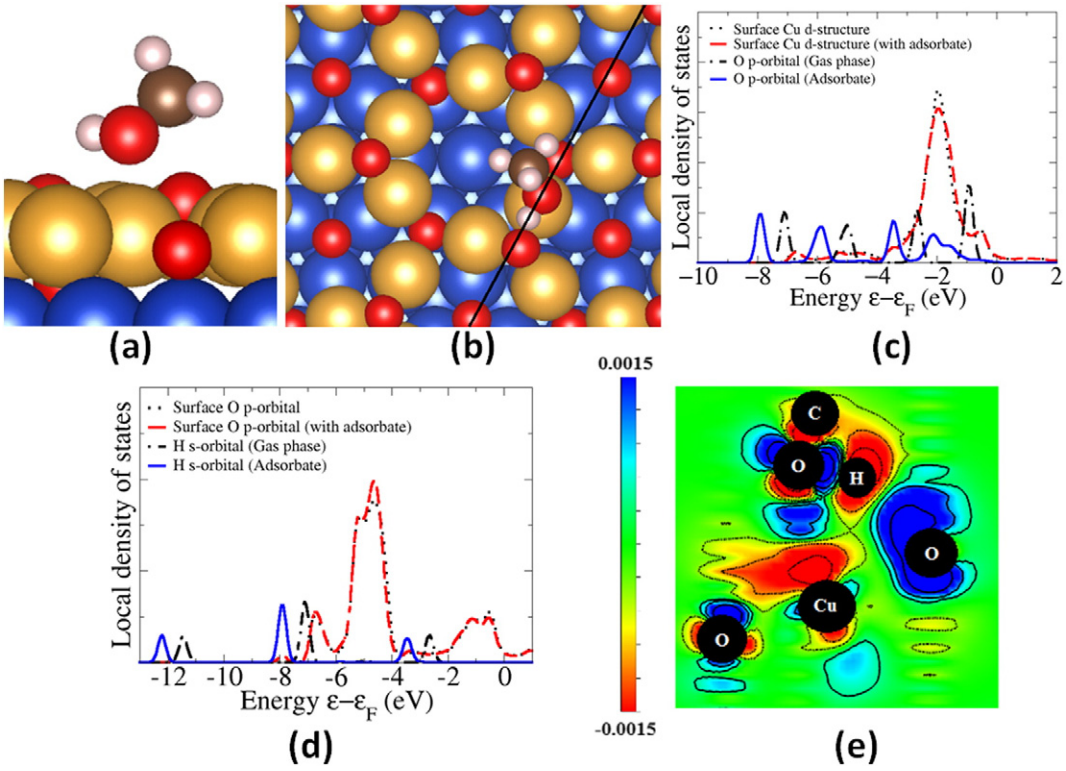

Fig. 2. Methanol adsorbed on the $Cu_2O/Cu(111)$ layer. (a) The side and (b) top views are shown of the molecule on the surface. (c) The local density of states plot of the O atom in methanol and the Cu atom it attaches to on the surface. (d) The local density of states plot of the H atom in methanol of the hydroxyl bond and the O atom of the surface. The units for the density of states are in arbitrary units. (e) 2-D charge density difference plot (e/Bohr^3). The solid black line in (b) is the location of where the 2-dimensional cuts were made for the charge density difference plot.

means that there is strong interaction with the Cu atoms and that the molecule is chemisorbed, rather than physisorbed as methanol is. Fig. 4(d) shows the charge density difference plot for methoxy on the Cu bridge site. Charge accumulation is observed on the O atom of methanol and the charge depletion is observed on the Cu atoms, showing strong interaction between the oxygen atom and the two Cu atoms. The Cu_2O monolayer lowers the stability of methoxy compared to the clean Cu(111) surface. We conclude that methoxy is a chemisorbed species on both Cu(111) and $Cu_2O/Cu(111)$ based on its bond distance, adsorption energy and electronic structure change.

3.2.3. Hydroxymethyl (CH_2OH)

The adsorption of hydroxymethyl is quite different from that of methanol. The molecule bonds by its carbon atom to the top of a Cu atom in both clean Cu(111) and $Cu_2O/Cu(111)$, with the C–O bond slightly tilted from being parallel to the surface as seen in Fig. 5(a, b). The distance between the C atom and the Cu atom is very short and this interaction leads to a large adsorption energy of −1.51 eV and −1.36 eV on Cu(111) and $Cu_2O/Cu(111)$, respectively. The distances from the C and O atoms to the closest Cu atom on the surface are 2.07 Å and 2.87 Å for Cu(111) and 2.07 Å and 2.83 Å for $Cu_2O/Cu(111)$.

Fig. 5(c) shows the local density of states of the C atom in hydroxymethyl and the Cu atom that it bonds to. Although some of the peaks of the C atom are well defined, there is some peak broadening near the Fermi energy. The density of states of the Cu atom downshifted and narrowed. Similar to methanol adsorption, the H atom in the hydroxyl bond has short distance of 1.91 Å to the closest surface O atom. Fig. 5(d) shows the local density of states of the H atom in the hydroxyl bond of hydroxymethyl and the O atom of the $Cu_2O/Cu(111)$ below it. The plot shows that all the peaks retained their peak definition and remained close to their gas phase positions. The charge density difference plot is shown in Fig. 5(e). Charge accumulation on the C site and depletion on the nearest Cu atom is observed. Although the local density of states plot does not show that there was any significant bonding between the H atom and the surface O atom, the charge density difference plot and bond distance reveal that there is weak bonding. Hydroxymethyl is chemisorbed on $Cu_2O/Cu(111)$ and Cu(111) with a small bond distance and high adsorption energy. We also found that there may be a weak bond between the H atom of hydroxymethyl and a surface O atom of $Cu_2O/Cu(111)$ by observing the change of local density states as well as its small bond distance.

3.2.4. Formaldehyde (CH_2O)

Formaldehyde bonds by its oxygen atom to the top of a Cu atom in both clean Cu(111) and $Cu_2O/Cu(111)$, with the C–O bond slightly tilted from being parallel to the surface as seen in Fig. 6(a, b). The molecule is shown to be on its side, rather than having a flat configuration. The distance between the O atom and the Cu atom is fairly large and this interaction leads to a small adsorption energy of −1.92 eV and −0.92 eV on Cu(111) and $Cu_2O/Cu(111)$, respectively. The distances from the O and C atoms to the closest Cu atom on the surface are 2.37 Å and 3.23 Å for Cu(111) and 2.65 Å and 3.33 Å for $Cu_2O/Cu(111)$.

Fig. 6(c) shows the local density of states of the O atom in formaldehyde and the surface Cu atom that it bonds to. Although some of the peaks of the p-orbital of the O atom in adsorbed formaldehyde slightly shift, the peaks are still narrow and well defined, remaining close to their gas phase positions. The peak of the d-structure of the Cu atom that the formaldehyde bonds to maintains its shape and does not experience any shift. The charge density difference plot is shown in Fig. 6(e). There is some charge accumulation on the O atom of methanol and charge depletion on the Cu atoms. The observed interaction between the O and the Cu for formaldehyde is stronger than that of methanol but weaker than methoxy. Formaldehyde adsorbs on $Cu_2O/Cu(111)$ and Cu(111) with a high bond distance and low adsorption energy.

The geometric structures of methanol, methoxy, hydroxymethyl and formaldehyde are similar for both clean Cu(111) and $Cu_2O/Cu(111)$.

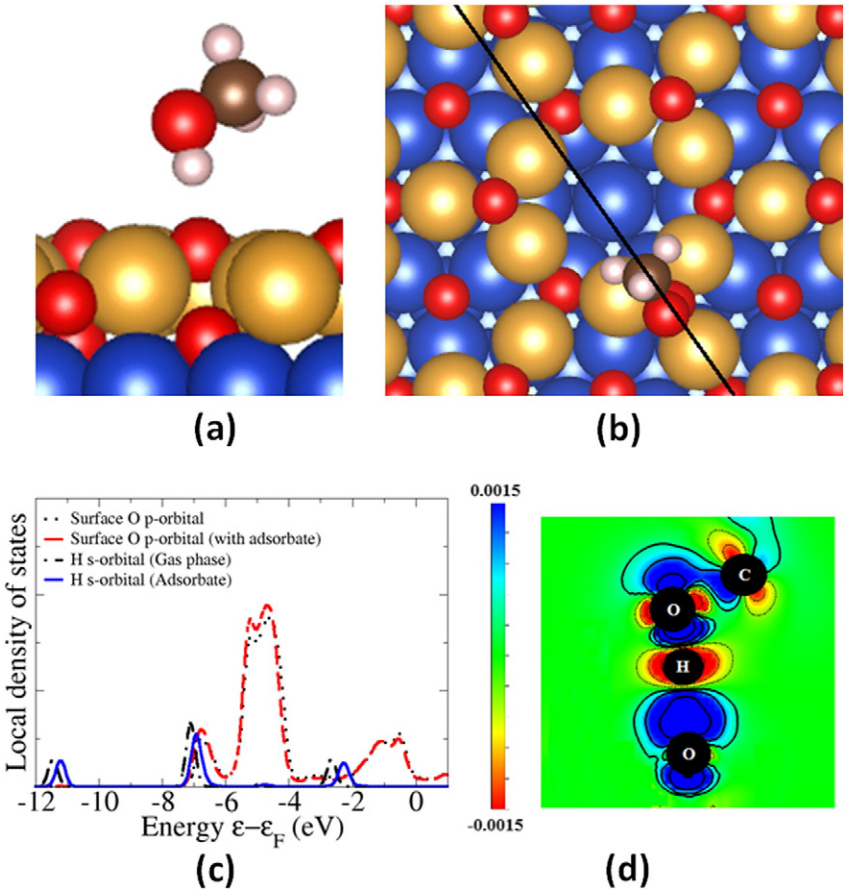

Fig. 3. H-adsorbed methanol adsorbed on the $Cu_2O/Cu(111)$ layer. (a) The side and (b) top views are shown of the molecule on the surface. (c) The local density of states plot of the H atom of the hydroxyl bond in methanol and the O atom it attaches to on the surface. (d) 2-D charge density difference plot (e/Bohr^3). The solid black line in (b) is the location of where the 2-dimensional cuts were made for the charge density difference plot.

Methanol and formaldehyde are adsorbed on top of a Cu atom for both surfaces, methoxy is strongly bonded to the fcc position of clean Cu(111) and bridge site for $Cu_2O/Cu(111)$, and hyrdroxymethyl is strongly adsorbed to the top of a Cu atom by its C atom, on both clean Cu(111) and also $Cu_2O/Cu(111)$ surfaces.

3.2.5. Hydrogen

We assume that a H atom will stay on the surface and form a hydroxyl bond (OH), after dissociating from the molecule. We calculated the most stable sites for the H atoms to reside, and they are on top of the two chemisorbed oxygen atoms of the $Cu_2O(111)$ layer. The adsorption energies for the H atoms on top of both the oxygen atoms are higher by 0.50 eV than any other adsorption site, so we can conclude that the H atoms will adsorb to the top of the chemisorbed O atoms after separating from the molecule, rather than the O atoms (i.e., lattice oxygen) within the Cu_2O monolayer.

The H adsorption energy is nearly identical for both the O atom located at the fcc or hcp sites. The location of the H atom on either fcc or hcp site after dissociation is chosen by relaxing the reaction intermediate on the surface while the H atom is on top of either chemisorbed oxygen atom. A H atom adsorbed at the hcp oxygen site is too close to the adsorbed methoxy, resulting in a spontaneous bonding back to methanol after relaxation, so we have to place the H atom at the fcc O site. For hydroxymethyl, the hydrogen adsorption energy is similar on either fcc or hcp O sites, so we choose to place the H on the fcc O site for consistency.

Although hydrogen is most stable on top of the chemisorbed oxygen atoms, we cannot neglect the possibility that a dissociated H will adsorb to a lattice O atom instead. If the dissociated H has to come into close contact with a lattice O atom, adsorption on the O atom may be a meta-stable state, and it may require a high energy barrier for a H atom to detach from a lattice O atom. If the energy barrier is relatively high, H adsorption on the lattice O can be considered as the stable site after decomposition. Although this situation did not occur, it may arise in future studies and it should be taken into account.

3.3. Methanol reactions

We studied dehydrogenation of both gas-phase and adsorbed methanol. Methanol decomposition does not require the assistance of an oxygen atom to promote dehydrogenation. In this study, the dissociated hydrogen atom is most stable on top of a chemisorbed oxygen atom, which is not the closest oxygen atom. The adsorbed methanol is far from the chemisorbed oxygen atom and is surrounded by closer oxygen atoms which the dissociated hydrogen atom does not attach to. For this reason, we consider the reaction of dehydrogenation of adsorbed methanol to be decomposition rather than oxidation.

Since the decomposition of methanol in our system results in a hydroxyl group, it may be mistaken for oxidation where the methanol interacts with the O atom. In our calculations, the dissociated H atom does bond with a chemisorbed O, methanol is already adsorbed to the surface before dehydrogenation, and the H atom also has to travel some distance to attach to the chemisorbed O atom, so we can still consider this reaction as decomposition. However, in our oxidation reactions, the chemisorbed O does directly interact with the molecule and plays a role in H dissociation as the gas phase methanol comes into close contact with the O atom.

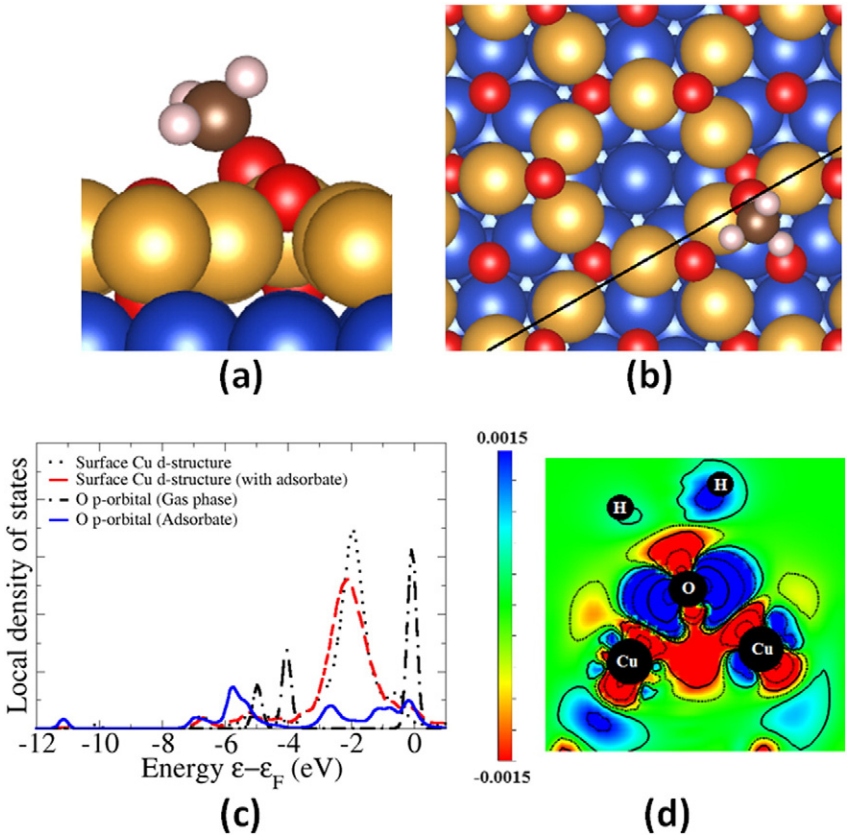

Fig. 4. Methoxy adsorbed on the $Cu_2O/Cu(111)$ layer. (a) The side and (b) top views are shown of the molecule on the surface. (c) The local density of states plot of the O atom in methoxy and the Cu atom it attaches to on the surface. The units for the density of states are in arbitrary units. (d) 2-D charge density difference plot (e/Bohr^3), where solid black line in (b) is the location of where the 2-dimensional cuts were made for the charge density difference plot.

3.3.1. C–H bond scission in methanol

Although the C–H bond scission in methanol has not been studied much in Cu systems, we calculated the C–H bond scission energy barrier to ensure that this is not the favorable initial reaction. Fig. 7(a) and (b) shows the O-adsorbed and H-adsorbed methanol before decomposition and Fig. 7(e) shows the final state after decomposition to hydroxymethyl. Table 2 lists our calculated energy barriers for methanol decomposition and oxidation on the $Cu_2O/Cu(111)$ layer and previously studied Cu(111). The scission occurs at the C–H bond and the H atom attaches to one of the chemisorbed O atoms. The activation energy is determined to be 1.98 eV for the scission of C–H bond in O-adsorbed methanol, and 1.85 eV for H-adsorbed methanol decomposition. Previous work in methanol decomposition on clean Cu(111) found this energy barrier to be 2.37 eV [17]. The breaking of the C–H bond in methanol is more favorable on the chemisorbed oxide layer than the clean Cu(111) layer. After the H atom dissociates from the methanol molecule, hydroxymethyl reorients itself to its most stable configuration as the H atom bonds to the chemisorbed O atom, as seen in Fig. 7(e). After C–H bond scission on $Cu_2O/Cu(111)$ occurs, the system becomes less stable than methanol adsorbed on the surface by 0.5 eV. During the reorientation of the hydroxymethyl, the H atom in the hydroxyl bond comes in close contact with an O atom that is part of the Cu_2O lattice. However, the H remains attached to the molecule, so the detachment of the H atom in the hydroxyl bond of hydroxymethyl during reorientation is not energetically favorable and unlikely to occur.

The dehydrogenation of gas-phase methanol is much more different than that of adsorbed methanol. In methanol decomposition, methanol starts as an adsorbed phase and loses a hydrogen atom, while oxidation involves interaction between methanol in its gas phase and a chemisorbed oxygen atom, causing a hydrogen atom to dissociate from methanol and then bonding with that oxygen atom. Fig. 7(c) shows the initial state of methanol in its gas phase before oxidation and Fig. 7(e) shows the final state after oxidation, where hydroxymethyl takes its most stable configuration and the hydrogen atom disassociates after interacting with the chemisorbed oxygen. The calculated energy barrier for oxidation on $Cu_2O/Cu(111)$ is 0.83 eV, which is lower than that of the decomposition, and 1.06 eV [17] lower than oxidation on a Cu(111) surface with an isolated oxygen atom. The chemisorbed oxygen atom assists in removing the hydrogen atom from the C–H bond in methanol by lowering the energy barrier for the bond breaking.

3.3.2. O–H bond scission in methanol

Methoxy after methanol decomposition is shown in its stable configuration in Fig. 7(d), and (a, b) shows the O-adsorbed and H-adsorbed methanol before decomposition. The scission occurs at the O–H bond, and like the case of hydroxymethyl, the H atom bonds to a chemisorbed O atom. The activation energy was determined to be 0.57 eV for this reaction for the O-adsorbed methanol and 2.78 eV for the H-adsorbed methanol. The energy barrier for the H-adsorbed methanol decomposition is relatively high. This high energy barrier is not due to the dissociation of the H atom, but is actually the saddle point in our NEB calculations where the surface structure is fairly distorted. Due to this surface distortion and high energy barrier, we conclude that H-adsorbed methanol decomposition to methoxy is not favorable and it is much more likely that decomposition would begin with the O-adsorbed methanol rather than the H-adsorbed methanol configuration. It should be noted that the H-adsorbed methanol is less stable than the O-adsorbed methanol, giving further evidence that decomposition of H-adsorbed methanol is less likely.

Our calculated energy barrier for decomposition of O-adsorbed methanol is in the range of values found by previous calculations on methanol decomposition between 0.25 [54] and 0.64 eV [17]. After the

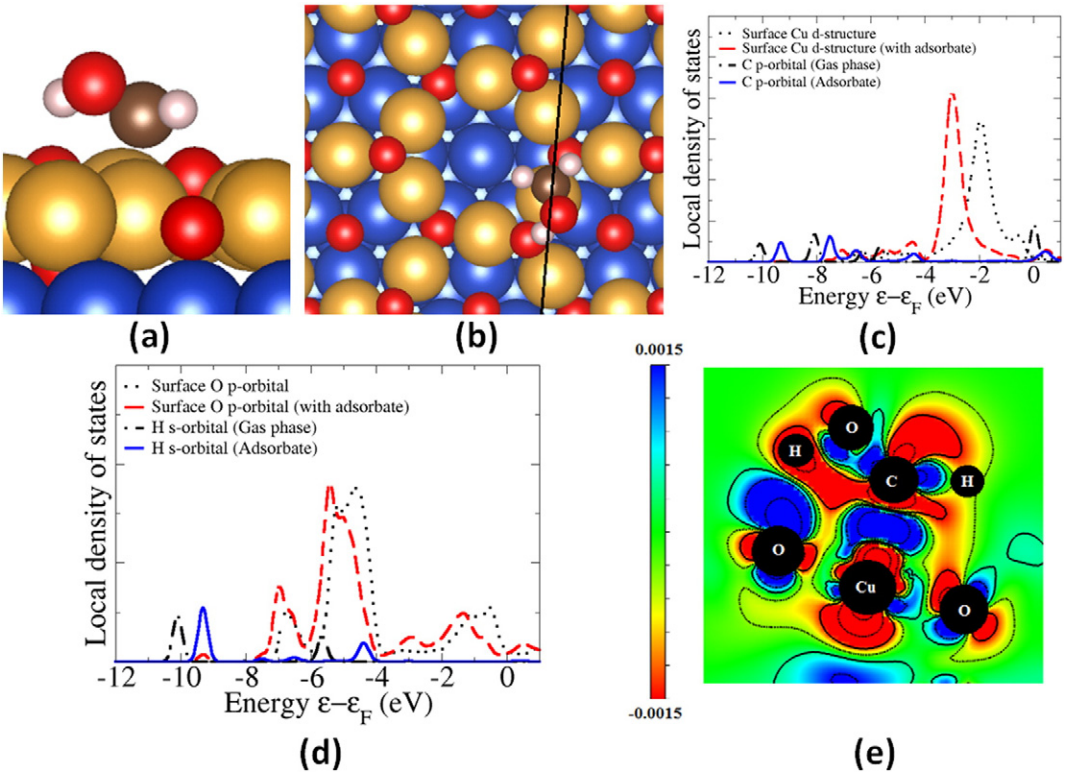

Fig. 5. Hydroxymethyl adsorbed on the $Cu_2O/Cu(111)$ layer. (a) The side and (b) top views are shown of the molecule on the surface. (c) The local density of states plot of the O atom in hydroxymethyl and the Cu atom it attaches to on the surface. (d) The local density of states plot of the H atom in the hydroxyl bond of methanol and the surface O atom underneath it. The units for the density of states are in arbitrary units. (e) 2-D charge density difference plot (e/Bohr^3), where the black line in (b) is the location of where the 2-dimensional cuts were made for the charge density difference plot. There is a H atom behind the C atom that is not shown on the charge plot, but its charge depletion is shown in between the C and Cu atom.

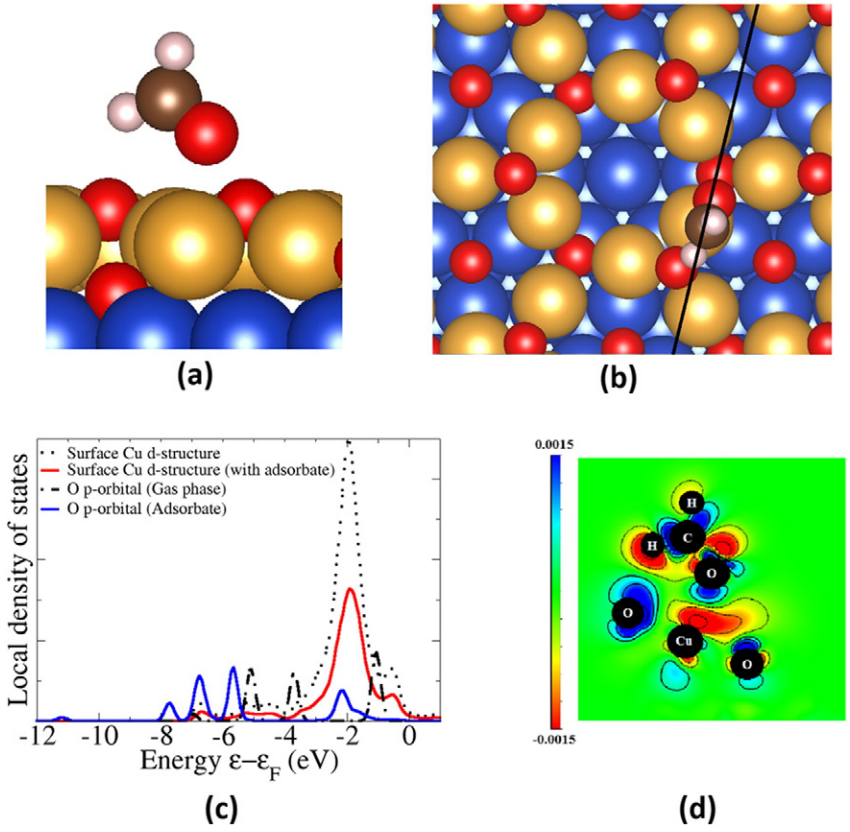

Fig. 6. Formaldehye adsorbed on the $Cu_2O/Cu(111)$ layer. (a) The side and (b) top views are shown of the molecule on the surface. (c) The local density of states plot of the O atom in formaldehyde and the Cu atom it attaches to on the surface. (d) 2-D charge density difference plot (e/Bohr^3), where the black line in (b) is the location where the 2-dimensional cuts were made for the charge density difference plot.

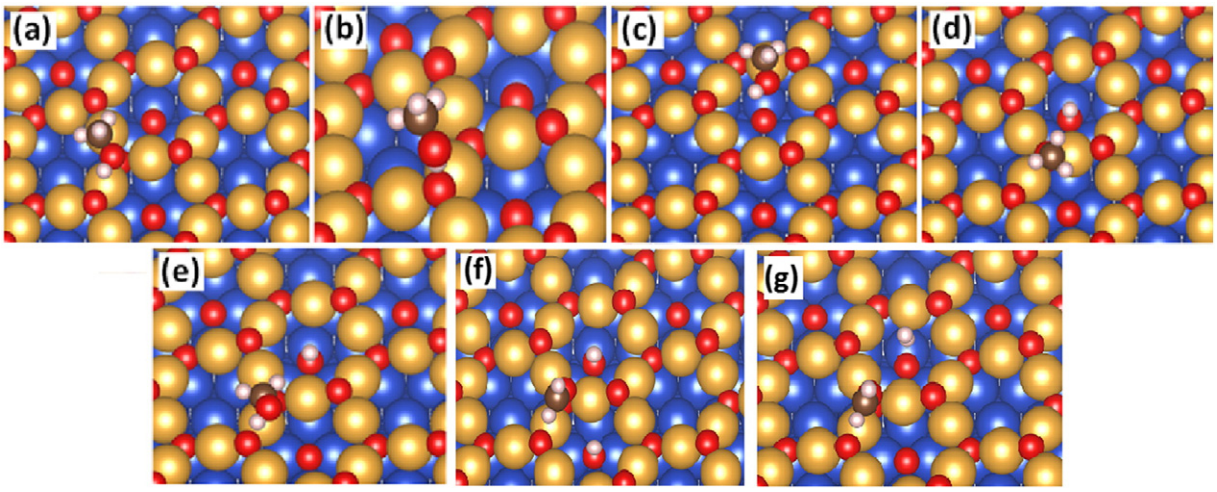

Fig. 7. Partial oxidation of methanol to formaldehyde: (a) the initial state of O-adsorbed methanol before dehydrogenation, (b) the initial state of H-adsorbed methanol before dehydrogenation, (c) the initial state of methanol in its gas phase before interacting with the oxygen atom directly below it, (d) the final state of the reaction with methoxy adsorbed and a hydrogen atom attached to the chemisorbed oxygen, (e) the final state of the reaction with hydroxymethyl adsorbed and a hydrogen atom attached to the chemisorbed oxygen, (f) the final state of formaldehyde and two adsorbed hydroxyl bonds and (g) the final state of formaldehyde and hydrogen molecule. The view is perpendicular to the surface with a slight tilt.

hydrogen atom dissociates from the hydroxyl bond, the methoxy reorients itself to its stable configuration. An adsorbed methoxy molecule and hydrogen atom on oxygen atom is more stable than hydroxymethyl and a chemisorbed hydrogen atom by 0.16 eV. The activation barrier for the O–H bond scission is also lower than the C–H bond scission of O-adsorbed methanol by 1.42 eV, making the O–H bond scission much more favorable in the first step of methanol decomposition.

Fig. 7(c) shows the initial state of methanol in its gas phase before oxidation and Fig. 7(d) shows methoxy after oxidation. We found this reaction to occur spontaneously. As the methanol molecule approaches the surface and passes by the chemisorbed O on its way to adsorbing to the Cu_2O/Cu(111) surface, the H atom from the hydroxyl bond comes into close contact with the chemisorbed O and breaks off without any energy barrier. Previous studies have shown that the O–H bond on methanol is spontaneously broken on the oxygen covered Cu(110) surface during optimization [15,17], which agree with our results where oxygen causes methanol oxidation to occur spontaneously. Another study found that the energy barrier for methanol oxidation to methoxy was significantly reduced to 0.17 eV, from 0.64 eV, on Cu(111) [19]. Since the energy barriers of O–H bond scission are much less than that of C–H bond scission in methanol, we do not further investigate hydroxymethyl as C–H bond scission is not the favorable initial reaction.

3.3.3. C–H bond scission in methoxy

The transition from methoxy to formaldehyde is known to be the rate-limiting step in methanol oxidation. Formaldehyde is shown in its stable configuration in Fig. 7(f, g). After the C–H bond scission of methoxy occurs, the hydrogen atom bonds to a chemisorbed O atom or bonds to another hydrogen atom to form the hydrogen molecule. In the latter case, the hydroxyl bond was formed from the previous reaction. When a hydrogen atom is placed on top of the hydroxyl bond, the hydrogen molecule is formed and separates from the chemisorbed oxygen atom.

The activation energy was determined to be 0.83 eV for the transition of methoxy to formaldehyde and two hydroxyl bonds, compared with 1.22 eV for the transition of methoxy to formaldehyde and the hydrogen molecule. We believe that the reaction barrier is lower to form two hydroxyl bonds due to the shorter distance between the dissociated hydrogen atom of methoxy and the chemisorbed oxygen atom, promoting the dehydrogenation with a stronger attractive force. To form the hydrogen molecule, the dissociated hydrogen atom has to travel further to bond with the hydrogen atom in the hydroxyl bond. The energy barriers for methoxy to form formaldehyde are still greater than any barrier that methanol has to overcome to form methoxy. From Table 2, we can see that the chemisorbed oxygen atom played a large role in promoting the dehydrogenation of methoxy to form formaldehyde.

As methanol partially oxidizes to form methoxy and then formaldehyde, the C–H bond scission of methoxy has the higher energy barrier. It takes more energy for methoxy to form formaldehyde and a hydrogen molecule than it is to form formaldehyde and another hydroxyl bond. While the previous study showed that an isolated atom on clean Cu(111) can reduce the methanol oxidation barrier, our results showed that a chemisorbed oxygen layer on Cu(111) makes the reaction occur spontaneously, indicating a clear difference between an oxygen covered surface and a chemisorbed oxygen layer in regards to methanol oxidation.

Table 2
The calculated energy barriers for methanol decomposition and oxidation to methoxy and hydroxymethyl. For decomposition, (O/H) signifies the energy barrier values for the initial state as O-adsorbed methanol and H-adsorbed methanol, respectively.

Reaction (adsorbed)	Cu_2O/Cu(111)	Clean Cu(111)
$CH_3OH + O$ to CH_3O (O/H)	0.57/2.78	0.64[a], 0.25[b]
$CH_3OH + O$ to CH_2OH (O/H)	1.98/1.85	2.37[a]
$CH_3O + OH$ to $CH_2O + H_2 + O$	1.22	–
$CH_3O + O$ to $CH_2O + OH$	0.87	1.65[a]
Reaction (initial gas phase)	Cu_2O/Cu(111)	Clean(111)with isolated O atom
$CH_3OH + O$ to $CH_3O + OH$	–	0.17[a]
$CH_3OH + O$ to $CH_2OH + OH$	0.83	1.89[a]

[a] Ref. [19].
[b] Ref. [67].

4. Conclusion

By employing DFT calculations, we have determined a stable Cu_2O/Cu(111) structure and the energetics of methanol, methoxy, hydroxymethyl and formaldehyde adsorption on the Cu_2O/Cu(111) layer and Cu(111) surface. The Cu_2O/Cu(111) structure resembles a Cu_2O monolayer on Cu(111) with chemisorbed O atoms on the hcp and fcc sites of the 2nd outermost layer. We also determined the activation energy for methanol to decompose and oxidize to methoxy and hydroxymethyl. Our results show close similarity of methanol, methoxy and hydroxymethyl geometric structures between Cu_2O/Cu(111) and clean Cu(111). Methanol is physisorbed as two configurations,

O-adsorbed and H-adsorbed, while both methoxy and hydroxymethyl are chemisorbed. According to our calculations, O–H scission is favorable over C–H scission in adsorbed and gas-phase methanol on Cu_2O/Cu(111). The chemisorbed O atom assists in methanol oxidation as the O–H bond spontaneously breaks without an energy barrier, and also lowers the C–H bond scission energy barrier. Methanol decomposes to methoxy more easily than hydroxymethyl, as expected. The chemisorbed oxygen layer plays an important role in methanol reactions, as it assists in hydrogen dissociation by lowering the energy barrier and the lattice and chemisorbed O atoms within the vicinity of the surface methanol and methoxy provide stable binding sites for the dissociated hydrogen atoms.

Acknowledgments

This work was supported by the National Science Foundation under NSF Collaborative Research Award Grant CBET-1264940. This work used the computational resources from the Extreme Science and Engineering Discovery Environment (XSEDE), which is supported by the National Science Foundation grant number OCI-1053575.

Appendix A. Supplementary data

Supplementary data to this article can be found online at http://dx.doi.org/10.1016/j.susc.2015.11.012.

References

[1] G. Wu, T. Chen, W. Su, G. Zhou, X. Zong, Z. Lei, C. Li, Int. J. Hydrog. Energy 33 (2008) 1243.
[2] Y. Huang, X. He, Z.X. Chen, J. Chem. Phys. 138 (2013) 184701.
[3] A.Y. Rozovskii, G.I. Lin, Top. Catal. 22 (2003) 137.
[4] J.C. Brown, E. Gulari, Catal. Commun. 5 (2004) 431.
[5] A. de Lucas-Consuegra, J. Gonzalez-Cobos, Y. Garcia-Rodriquez, A. Mosquera, J.L. Endrino, J.L. Valverde, J. Catal. 293 (2012) 149.
[6] Y.J. Huang, K.L. Ng, H.Y. Huang, Int. J. Hydrog. Energy 36 (2011) 23.
[7] R.M. Navarro, M.A. Pena, J.L.G. Fierro, J. Catal. 212 (2002) 112.
[8] P. Lopez, G. Mondragon-Galicia, M.E. Espinosa-Pesqueria, D. Mendoza-Anaya, M.E. Fernandez, A. Gomez-Cortes, J. Bonifacio, G. Martinez-Barrera, R. Perez-Hernandez, Int. J. Hydrog. Energy 37 (2012) 11.
[9] A. Haghofer, K. Fottinger, F. Girgsdie, D. Teschner, A. Knop-Gericke, R. Schlogl, G. Rupprehter, J. Catal. 286 (2012) 13.
[10] D.R. Palo, R.A. Dagle, J.D. Holladay, Chem. Rev. 107 (2007) 3992.
[11] K.M. Vanden Bussche, G.G. Froment, J. Catal. 161 (1996) 1.
[12] X.K. Gu, W.X. Li, J. Phys. Chem. C 114 (2010) 21539.
[13] T.-J. Huang, S.-W. Wang, Appl. Catal. 24 (1986) 287.
[14] H. Oguchi, H. Kanai, K. Utani, Y. Matsumura, S. Imamura, Appl. Catal. A 293 (2005) 64.
[15] S. Sakong, A. Grob, J. Catal. 231 (2005) 420.
[16] S. Sakong, C. Sendner, A. Grob, J. Mol. Struct. 771 (2006) 117.
[17] S. Sakong, A. Gross, J. Phys. Chem. C 111 (2007) 8814.
[18] J.R.B. Gomes, J.A.N.F. Gomes, Surf. Sci. 471 (2001) 59.
[19] Z.J. Zuo, L. Wang, P.D. Han, W. Huang, Int. J. Hydrog. Energy 39 (2014) 1664.
[20] J. Greeley, J.K. Norskov, M. Mavrikakis, Annu. Rev. Phys. Chem. 53 (2002) 319.
[21] K. Nakatsuji, M. Hu, Int. J. Quantum Chem. 77 (2000) 341.
[22] I.E. Wachs, J. Madix, J. Catal. 53 (1978) 208.
[23] M. Bowker, J. Madix, Surf. Sci. 95 (1980) 190.
[24] R.J. Madix, S.G. Telford, Surf. Sci. 328 (1995) L576.
[25] P. Boulet, A. Baiker, H. Chermetter, F. Gilardoni, J.-C. Volta, J. Weber, J. Phys. Chem. B 106 (2002) 9659.
[26] C.-Q. Lv, C. Liu, G.-C. Wang, Catal. Commun. 45 (2014) 83.
[27] T. Matsumoto, R.A. Bennett, P. Stone, T. Yamada, K. Domen, M. Bowker, Surf. Sci. 471 (2001) 225.
[28] F. Jensen, F. Besenbacher, E. Laegsgaard, I. Stensgaard, Surf. Sci. 259 (1991) L774.
[29] F. Jensen, F. Besenbacher, I. Stensgaard, Surf. Sci. 270 (1992) 400.
[30] G. Zhou, X. Chen, D. Gallagher, J.C. Yang, Appl. Phys. Lett. 93 (2008).
[31] G. Ertl, Surf. Sci. 6 (1957) 208.
[32] A. Spitzer, H. Luth, Surf. Sci. 118 (1982) 136.
[33] R.W. Judd, P. Hollins, J. Pritchard, Surf. Sci. 171 (1986) 643.
[34] M.K. Rajumon, C.N.R.R.K. Prabhakaran, Surf. Sci. 233 (1990) L237.
[35] R.L. Toomes, D.P. Woodruff, M. Polcik, S. Bao, P. Hofmann, K.M. Schindler, Surf. Sci. 443 (2000) 300.
[36] S.M. Johnston, A. Mulligan, V. Dhanak, M. Kadodwala, Surf. Sci. 518 (2002) 57.
[37] Y. Xu, M. Mavrikakis, Surf. Sci. 494 (2001) 131.
[38] A. Soon, M. Todorova, B. Delley, C. Stampfl, Phys. Rev. B 73 (2006) 165424.
[39] A. Soon, M. Todorova, B. Delley, C. Stampfl, Phys. Rev. B 75 (2007) 125420.
[40] A. Soon, M. Todorova, B. Delley, C. Stampfl, Surf. Sci. 601 (2007) 5809.
[41] F. Yang, Y.M. Choi, P. Lui, D. Stacchiola, J. Hrbek, J.A. Rodriquez, J. Am. Chem. Soc. 133 (2011) 11474.
[42] G. Kresse, J. Hafner, Phys. Rev. B 47 (1993) 558.
[43] G. Kresse, J. Hafner, Phys. Rev. B 49 (1994) 14251.
[44] G. Kresse, J. Furthmüller, Comput. Mater. Sci. 6 (1996) 15.
[45] G. Kresse, J. Furthmüller, Phys. Rev. B 54 (1996) 11169.
[46] J.P. Perdew, K.A. Jackson, M.R. Pederson, D.J. Singh, C. Fiolhais, Phys. Rev. B 46 (1992) 6671.
[47] J.P. Perdew, Y. Wang, Phys. Rev. B 33 (1986) 8800.
[48] G. Kresse, D. Joubert, Phys. Rev. B 59 (1999) 1758.
[49] P.E. Blöchl, Phys. Rev. B 50 (1994) 17953.
[50] J. Greeley, M. Mavrikakis, J. Am. Chem. Soc. 126 (2004) 3910.
[51] Z.R. Xiao, G.Y. Guo, J. Chem. Phys. 130 (2009) 214704.
[52] H.J. Monkhorst, J.D. Pack, Phys. Rev. B 13 (1976) 5188.
[53] M. Methfessel, A. Paxton, Phys. Rev. B 40 (1989) 3616.
[54] T. Kangas, K. Lassonen, A. Puisto, H. Pitkanen, M. Alatalo, Surf. Sci. 584 (2005) 62.
[55] S.Y. Liem, G. Kresse, J.H.R. Clarke, Surf. Sci. 415 (1998) 194.
[56] L. Li, Q.Q. Li, J. Li, W.A. Saidi, G.W. Zhou, J. Phys. Chem. C 118 (2014) 20858.
[57] G. Henkelman, B.P. Uberuaga, H. Jonsson, J. Phys. Chem. C 113 (2000) 9901.
[58] Z. Riguang, L. Hongyan, L. Lixia, L. Zhong, W. Baojun, Appl. Surf. Sci. 257 (2011) 4243.
[59] M. N'dollo, P.S. Moussounda, T. Dintzer, F. Garin, J. Mod. Phys. 4 (2013) 409.
[60] H. Wang, C.Z. He, L.Y. Huai, J.Y. Liu, J. Phys. Chem. C 117 (2013) 4574.
[61] K. Momma, F. Izumi, J. Appl. Crystallogr. 41 (2008) 653.
[62] K. Momma, F. Izumi, J. Appl. Crystallogr. 44 (2011) 1271.
[63] F. Yang, Y. Choi, P. Liu, J. Hrbek, J.A. Rodriguez, J. Phys. Chem. C 114 (2010) 17042.
[64] C.T. Vo, L.K. Huynh, J.Y. Hung, J.C. Jiang, Appl. Surf. Sci. 280 (2013) 219.
[65] M. Calatayud, J. Andrés, A. Beltrán, Surf. Sci. 430 (1999) 213.
[66] G. Carchini, N. López, Phys. Chem. Chem. Phys. 16 (2014) 14750.
[67] J. Greeley, M. Mavrikakis, J. Catal. 208 (2002) 291.